

UAV BORNE MAPPING BY MULTI SENSOR INTEGRATION

Masahiko Nagai, Tianen Chen, Afzal Ahmed, Ryosuke Shibasaki

Centre for Spatial Information Science
The University of Tokyo, Japan,
435 Research Centers, CSIS, 5-1-5 Kashiwanoha, Kashiwa, Chiba 277-8568, Japan
Tel: +81-4-7136-4307 Fax: +81-4-7136-4292;
nagaim@iis.u-tokyo.ac.jp

ThS-23: UAV for Mapping

KEY WORDS: Laser Scanning, CCD, IMU, Calibration, Mobile, Platform.

ABSTRACT:

Three dimensional data is in great demand for disaster and environmental monitoring. In order to represent 3D space in details, it is indispensable to acquire 3D shape and texture together efficiently. However, they still lack a reliable, quick, cheap and handy method of acquiring three dimensional data of objects at higher resolution and accuracy in outdoors and moving environments. In this research, utilization of UAV (Unmanned Aerial Vehicle) is proposed. UAV is often used in military purpose, but also UAV is currently used in civil purpose such as mapping and disaster monitoring. UAV can fly lower altitude to get precise information and it is good for dangerous situation, however UAV has some limitations in terms of payload. It is difficult to mount aerial remote sensing sensors, so UAV mapping is still at the level of monitoring, not at the level of surveying. In this research, a combination of CCD cameras and a small (cheap) laser scanner with inexpensive IMU and GPS is proposed for an UAV borne 3D mapping system. Direct geo-referencing is achieved automatically using all the sensors without any ground control points. A new method of direct geo-referencing by the combination of bundle block adjustment and Kalman filter is proposed. This is the way of rendering objects with rich shape and detailed texture automatically by using an UAV.

1. INTRODUCTION

Aerial survey has become very valuable method for mapping and environmental monitoring. Remote sensors, such as an image sensor or a laser scanner, gather information about an object or area from a distance. Recently, some high resolution sensors has been developed for various purpose. They can cover widely target area and also archived data is available for users, but the spatial and temporal resolution is not always enough for detailed mapping.

Field workers use to conduct ground survey by using an instrument called a total station (a small telescope equipped with an electronic distance measuring device), GPS, a laser scanner, digital camera and so on. Ground surveying is conducted on the ground, so generally it is very close to, or on, observation targets. Therefore, they can get detailed and accurate information, but these techniques take a lot of labors and expenses, and spending times for the surveying. Also, it is not always safety in the case of the stricken area.

UAV borne mapping system is developed as an intermediate mapping system between aerial survey and ground survey in terms of coverage and spatial resolution. All the measurement tools are mounted on the UAV to acquire detailed information from low altitude which is different from a satellite or a plane. The survey is carried from the sky, but the resolution and accuracy are the same level of the ground surveying. The data can be easily acquired collectively with safety and mobility by the utilization of an UAV.

In this research, a combination of a CCD camera and a small (cheap) laser scanner with an inexpensive IMU (Inertial

Measurement Unit) and GPS for mobile platform are proposed. The method to integrate these sensors should be developed for the high precision positioning system in moving environment (Nagai and Shibasaki, 2006). In this research, the way of direct geo-referencing is achieved automatically from mobile platform without any ground control points. Here, direct geo-referencing means geo-referencing which do not require ground control points with accurately measured ground coordinate values. The methods of data acquisition and digital surface model are developed with the method of direct geo-referencing of laser range data and CCD camera with GPS and IMU from an UAV.

2. SYSTEM DESIGN

2.1 Sensors

In this research, laser scanner and CCD cameras (digital camera and IR camera) with IMU and GPS are used to construct digital surface model. In order to construct digital surface model automatically, it is necessary to develop the high precision positioning system in all circumstances for determining the movement of sensors. Integration of GPS/IMU is very effective for high accuracy positioning of mobile platform. 3D shape is acquired by laser scanner as point cloud data, texture information is acquired by digital camera, and vegetation indexes are acquired by IR camera from the same platform simultaneously. List of sensors which is used in this research is shown in Table 1.

The key points of the system design are to realize "Handiness" and "Mobility" of the system. "Handiness" means low cost, easy method and process. Utilization of a small laser scanner, a

commercial digital camera, and an inexpensive IMU (FOG: Fiber Optic Gyro) are proposed for multi sensor integration, and these sensors are low cost in comparison with existing aerial measurement system. These low cost equipments are easy to find in market. "Mobility" means light weight system and simple system to modify. Weights of sensors are shown in Table 1. That is, this system can be borne by a variety of platforms, any kinds of UAV, and not only an UAV but also ground vehicle, carrying by human, etc. These sensors do not own excellent specification, but they are light and low cost with enough specification. These handy sensors are used and make excellent results by integrating of sensors.

Sensors	Model	Specification
Digital Camera	Canon EOS 10D	3,072×2,048 pixels Focus length: 24.0mm Weight: 500g
Digital Camera	Canon EOS 5D	4,368×2,912 pixels Focus length: 15.0mm (Fish eye lens) Weight: 500g
IR Camera	Tetracam ADC3	2,048×1,536 pixels Green, Red and NIR sensitivity with bands approximately equal to TM2, TM3 and TM4. Focus length: 10.0mm Weight: 500g
Laser Scanner	SICK LMS-291	Angular resolution: 0.25° Max. Distance: 80m Accuracy (20m) : 10mm Weight: 4,000g
IMU	Tamagawa Seiki Co., Ltd TA7544	Fiber Optic Gyro Accuracy Angle: ±0.1° Angle Velocity: ±0.05°/s Acceleration: ±0.002G Weight: 1,000g
GPS	Ashtech G12	Accuracy Differential: 40cm Velocity Accuracy: 0.1(95%) Weight: 150g

Table 1. List of sensors

2.2 UAV Platform

In this research, all the measurement tools are mounted on the UAV, RPH2, which is made by Fuji Heavy Industries Ltd., shown in Figure 1. The size of RPH2 is a length of 4.1m, a width of 1.3m, and a height of 1.8m and weight is 330kg. Payload is approximately 100kg. All the sensors are tightly fixed under the UAV. RPH2 is quite big UAV, however, in this study, RPH2 is considered as testbed which is a platform for experimentation for development of multi sensor integration algorithm. RPH2 has large payload, so many sensors and control PCs with large battery can be mounted during experiment. After the development of the multi sensor integration algorithm, small UAV system, as shown in Figure 2 is implemented with selected sensors for certain observation target.

There are several advantages to utilize an UAV. One of the most advantageous things is unmanned platform, so it can fly over dangerous zone such as disaster, floating ice, land mines, and so on. Advantage of UAV suits the purpose of direct geo-referencing of this research. Direct geo-referencing does not require ground control points with accurately measured ground

coordinate value. In dangerous zone, it is impossible to set control points unlike normal aerial surveys. Therefore, combination of this direct geo-referencing method from an UAV might be ideal tools for dangerous monitoring purpose. Therefore, the targets of this mapping system are for disaster such as landslide and river monitoring, not for urban area.

In addition, for conducting safety operation, the UAV is restricted to fly over people, houses, and cars, also, the UAV doesn't fly if wind speed is more than 10 m/s. In the experiment, the UAV flies about 1.6m/sec. of speed for acquiring laser point data with sufficiently fine resolution and sequential digital camera images with sufficient overlaps.



Figure 1. RPH2



Figure 2. Small UAVs

2.3 Setting of Sensors

All the sensors are tightly fixed on the UAV to have constant geometric relationship. Calibration of CCD cameras is calculated for interior orientation parameters such as focal length, lens, distortion, principle points, and interior orientation (Kunii and Chikatsu, 2001). Estimation of relative position and attitude among the sensors is also conducted (Shapiro, 1987). All the sensors are controlled by one laptop PC and they are synchronized by GPS time (one pulse per second). Sensors are set as shown in Figure 3. Digital video camera is also put on the UAV. This video camera sends images to the ground on real time to monitor flight course. RPH2 has large payload, so it is not necessary to think about weight. Large battery is also set to supply sensors and PC with electric power during the experiment. It is possible to flight long period.

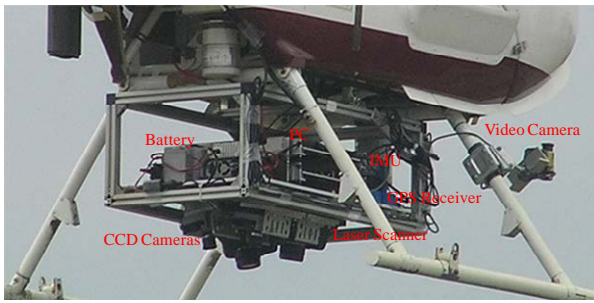


Figure 3. Setting of sensors

3. MULTI SENSOR INTEGRATION

3.1 Overview of Sensor Integration

Figure 4 shows the overview of data processing. In this research, following data are acquired; base station GPS data, remote station GPS data, IMU data, CCD images, and laser range data. Though the data are acquired in different frequencies, they are synchronized each other by GPS time.

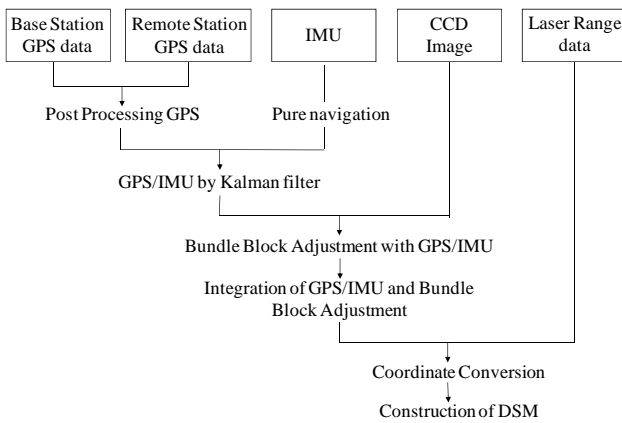


Figure 4. Sensor integration

At first, differential GPS post processing is conducted by Waypoint's GrafNav commercial software with accuracy of approximately 30cm. Secondly, processed GPS data and IMU data are integrated by Kalman filter operation. Thirdly, bundle block adjustment of CCD images is made with the support of GPS/IMU. Finally, GPS/IMU and the result of bundle block adjustment are combined to generate high precision and time series position and attitude. Then, this hybrid positioning data is used for coordinate conversion of laser range data and construction of digital surface model.

3.2 Multi Cameras

In order to cover wide area from low altitude, multi cameras are mounted on the UAV. In this study, two digital cameras and two IR cameras are mounted in parallel with some angles. These CCD cameras are tightly fixed on the iron plate to have constant geometric relationship during experiment as shown in Figure 5.

Four images are acquired at the same time, as shown in Figure 6. Those images are mosaicked by using calibration data and result of image orientation. Rectified images are mosaicked by

GPS data. Image overlap is estimated by GPS altitude information. Then, image matching of overlapped area is conducted and mosaic image is constructed. Mosaic images can cover more wide even though flight altitude is no so high. Fish-eye lens image is also acquired from the UAV to cover wide area as shown in Figure 7. The ground coverage from 50m altitude is 330m × 110m.



Figure 5. Multi camera setting

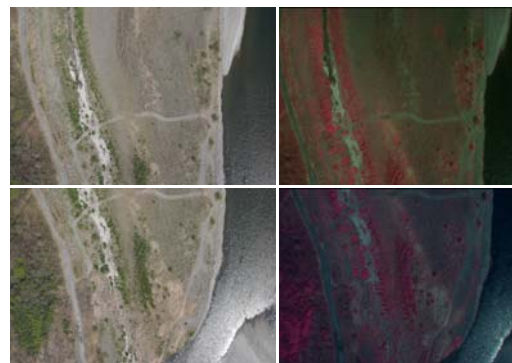


Figure 6. CCD Images by multi cameras



Figure 7. Fish-eye lens image

3.3 GPS/IMU integration by Kalman filter

The integration of GPS and IMU is implemented by using Kalman filter. The Kalman filter can be used to optimally estimate the system states. In the Kalman filter, the final estimation is based on a combination of prediction and actual measurement. The pure navigation algorithm is operated for IMU to calculate attitude, velocity, and position (Kumagai, et al., 2002). The navigation procedure proceeds step by step. Inertial navigation starts to define its initial attitude and heading. Then, its process changes to the navigation mode. IMU has a

rising quality, but it is still affected by systematic errors, which is called drift error. Here, GPS measurement is applied as actual measurement in order to aid IMU by correcting this huge drift error. Through Kalman filter operation, an optimal estimate of the sensor position and attitude is determined from GPS and IMU.

Figure 8 shows Kalman filter circulation diagram for GPS/IMU integration (Kumagai, et al., 2000). Individual measurement equations and transition equation are selected and the initialization of each covariance is necessary to continue the Kalman filter circulation in response to the GPS validation. Accuracy of GPS/IMU integration depends on accuracy of referenced GPS. In this case, it is approximately 30 cm.

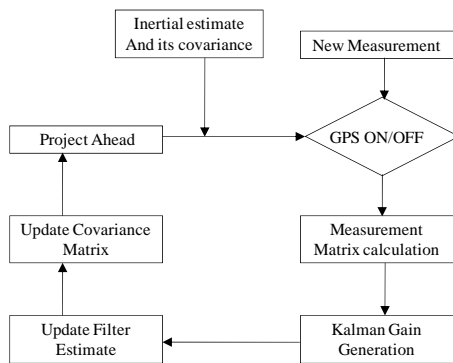


Figure 8. Kalman filter circulation diagram

In addition, boresight offset must be estimated between GPS and IMU, and also the other sensors. In the Kalman filter circulation, differences of position and velocity between IMU and GPS are used to estimate amount of errors in IMU. If the UAV just goes straight, amount of errors is not affected because the relative movement is constant. However, if the UAV makes a turn, amount of errors is not constant. Position and velocity of near axis of gyration is small, though its far axis of gyration is large. In this research, boresight offset from GPS to IMU in the UAV is obtained by direct measurement.

3.4 Bundle block adjustment of CCD images

Meanwhile, orientation of digital camera is determined by bundle block adjustment. Bundle block adjustment is a non linear least squares optimization method using tie-points of inside block. Bundle block adjustment is used for the determination of the orientation parameters of all CCD images (Takagi and Shimoda, 2004). Bundle block configuration increases both the reliability and the accuracy of object reconstruction. An object point is determined by intersection from more than two images, which provides local redundancy for gross error detection and which makes a better intersection geometry as a result (Chen, et al., 2003). So, in this research, CCD images are taken for more than 60% overlapping in forward direction, and more than 40% overlapping in side. GPS/IMU allows automatic setting of tie-points and it reduces searching time of tie-points by the limitation of searching area based on epipolar line. The epipolar line is the straight line of intersection of the epipolar plane with the image plane which is estimated by GPS/IMU. It connects the image point in one image through the image point in the next image.

Figure 9 shows a series of image orientation with tie points which overlapped each other. Resolution of those images is approximately 1.5cm. This is super high resolution image. So it is not difficult to detect small gaps or cracks.

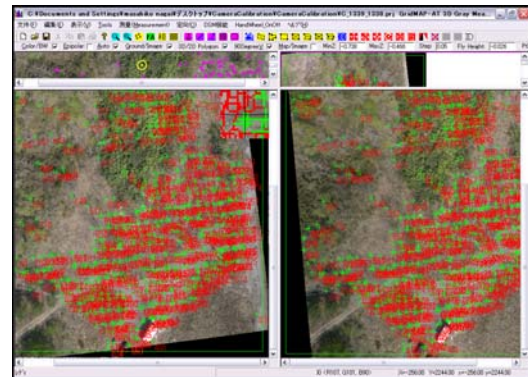


Figure 9. Image processing

Table 2 shows the result of bundle block adjustment. “cp” is the control points which is measured by total station as true values. “ba” is the computation result by bundle block adjustment. Accuracy is estimated by comparing 20 control points and the result of bundle adjustment. Average of residual of its plane (X, Y) is approximately 3cm to 6cm. Average of residual of its height (Z) is approximately 10cm. That is, this result is very accurate as compared with differential GPS or GPS/IMU integration. Therefore, the result of bundle block adjustment aids the Kalman filter by initialization of position and attitude.

Num	X(cp:m)	Y(cp:m)	Z(cp:m)	X(ba:m)	Y(ba:m)	Z(ba:m)	residual:X	residual:Y	residual:Z
1	0	0	-12.584	0.094	-0.059	-12.311	0.094	0.059	0.273
2	11.3105	0	-12.3825	11.293	-0.062	-12.48	0.0175	0.062	0.0975
3	20.8395	0.168	-12.4065	20.79	0.111	-12.515	0.0495	0.057	0.1085
4	32.588	0.2885	-12.441	32.527	0.229	-12.564	0.061	0.0595	0.123
5	46.196	0.5035	-12.5105	46.103	0.447	-12.518	0.093	0.0565	0.0075
6	0.074	-8.1735	-12.515	0.173	-8.145	-12.336	0.099	0.0285	0.179
7	11.3245	-7.905	-12.428	11.346	-7.891	-12.458	0.0215	0.014	0.03
8	20.5425	-7.703	-12.4345	20.525	-7.72	-12.499	0.0175	0.017	0.0645
9	30.677	-7.315	-12.406	30.622	-7.341	-12.575	0.055	0.026	0.169
10	46.7025	-7.81	-12.566	46.608	-7.849	-12.459	0.0945	0.039	0.107
11	0.4485	-14.9755	-12.473	0.551	-14.917	-12.378	0.1025	0.0585	0.097
12	11.6895	-15.058	-12.4075	11.734	-15.019	-12.483	0.0445	0.039	0.0755
13	20.3605	-14.902	-12.419	20.361	-14.891	-12.518	0.0005	0.011	0.099
14	30.447	-15.3555	-12.47	30.424	-15.347	-12.503	0.023	0.0085	0.033
15	46.3735	-15.455	-12.5715	46.289	-15.456	-12.401	0.0845	0.001	0.1705
16	0.3535	-24.139	-12.443	0.453	-24.072	-12.522	0.0995	0.067	0.079
17	11.911	-23.7855	-12.455	11.987	-23.721	-12.466	0.076	0.0645	0.011
18	20.594	-23.461	-12.453	20.623	-23.421	-12.507	0.029	0.04	0.054
19	30.176	-23.1665	-12.4505	30.165	-23.13	-12.491	0.011	0.0365	0.0405
20	46.258	-22.5005	-12.5545	46.2	-22.493	-12.39	0.058	0.0075	0.1645
						ave	0.05655	0.0376	0.09915

Table 2. Result of bundle block adjustment

3.5 Positioning by multi-sensor integration

The positioning and attitude of sensors are decided by integration of GPS/IMU, as well as CCD images. One of the main objectives of this research is to integrate sensors for developing the high precision positioning system by using inexpensive equipments. Integration of GPS, 1Hz, and IMU, 200Hz, has to be made with Kalman filter for geo-referencing of laser range data with the frequency of 18Hz. Positioning accuracy of GPS/IMU is approximately 30cm, because it is limited by the accuracy of GPS. On the other hand, position and attitude can be estimated for very high accurately with bundle block adjustment of CCD images, though the images are taken in every 10 seconds.

Therefore, the combination of bundle block adjustment and GPS/IMU by the Kalman filter is conducted to achieve higher

accuracy. The results of bundle block adjustment are assumed to be true position values. It provides initial attitude and heading without any alignments. IMU/GPS are initialized for the Kalman filter using the result of bundle block adjustment in ever 10 seconds. Namely, after every computation of bundle block adjustment, GPS/IMU and its error are corrected. Figure 10 is the strapdown navigation algorithm for integrating GPS/IMU with the result of bundle block adjustment. The combination of GPS/IMU and bundle block adjustment can be called "hybrid IMU".

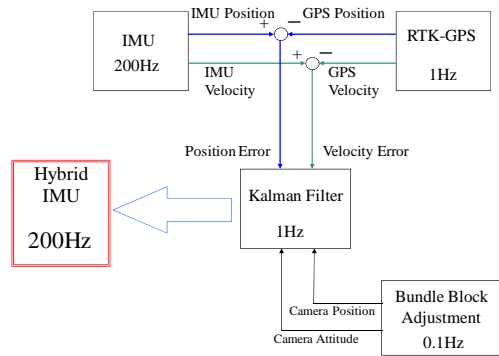


Figure 10. Strapdown navigation algorithm

As the result of GPS/IMU which is corrected with bundle block adjustment, trajectory of hybrid IMU can assure sufficient geo-referencing accuracy for the CCD images. The trajectory of digital camera can be representative of the trajectory of the platform because GPS/IMU is initialized by camera orientation. This is one of the advantages of this system. GPS/IMU coordinate is fitted to digital camera coordinate. Figure 11 shows the trajectory of the UAV in this experiment. Hybrid IMU is computed by aiding GPS/IMU and bundle block adjustment. The square dots are the timing of bundle block adjustment, GPS/IMU by the kalman filter is initialized by these points. The circle dots are the trajectory of GPS. The line is the Hybrid IMU, which is combined GPS/IMU and results of bundle block adjustment.

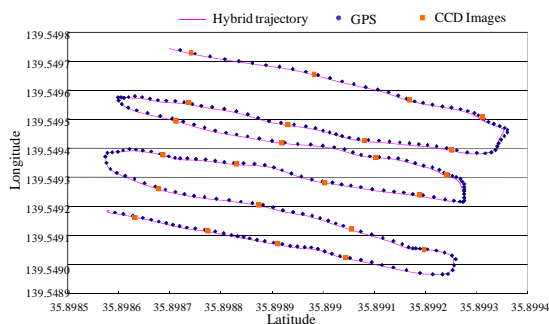


Figure 11. Trajectory of the UAV

4. DIGITAL 3D MODEL

4.1 Direct geo-referencing

While the measuring, the platform including all sensors is continuously changing its positions and attitudes with respect to

time. For direct geo-referencing of laser range data and CCD images, hybrid IMU which are integrated by GPS/IMU and bundle block adjustment is used. There are only two coordinate systems, laser scanner coordinate system and the common world coordinate system, are existing. GPS/IMU and bundle block adjustment of CCD images already have the common world coordinate system. That is, just laser scanner coordinate system must be converted to the common world coordinate system by geo-referencing. Geo-referencing of range data is determined by the 3D helmert's transformation which is computing rotation matrix and shift vector with hybrid IMU data and calibration parameters as offset. Offset from laser scanner to digital camera in body frame is already obtained by sensor calibration.

All the points scanned by the laser scanner (x) are converted to the common world coordinate system (Xw) which is the same as digital camera coordinate system as given in equation (1). Rotation matrix (Rh) and shift vector (Sh) from hybrid IMU which corrects drift error are used with respect to time. Offset values (RI-d and SI-d) are already estimated in sensor calibration.

$$X_w = (R_h * R_{I-d}) x + (S_h + S_{I-d}) \tag{1}$$

Where Rh, Sh : hybrid IMU, Rotation and Shift
RI-d, SI-d : offset by calibration

Geo-referencing of laser range data and CCD images is done directly. Figure 12 shows the 3D point cloud data which is directly geo-referenced by hybrid IMU data. In this research, the world coordinate system of CCD images is used as the base coordinate system, so all points have the world coordinate system.

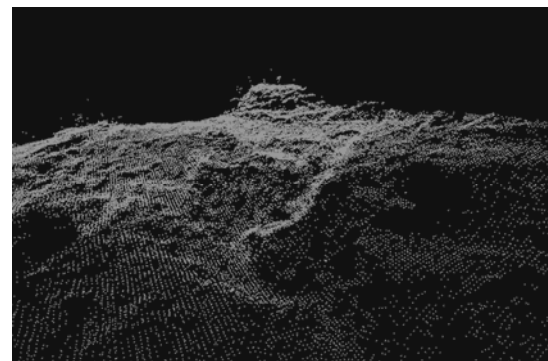


Figure 12. 3D point cloud data

4.2 Color rendering

The digital surface model, which is a 3D model of the object surface, is manipulated using a computer. It is comprised of 3D measurements that are laid out on colored points cloud. These measurements use the 3D point cloud data, which are derived from laser scanner, and texture data, which is derived from CCD sensors.

The point cloud data acquired by laser scanner is geo-referenced by hybrid IMU data. This hybrid IMU data is based on the common world coordinate system, which is the same as

the coordinate of CCD images. Texture data are overlaid on geo-referenced point cloud data. The integrated point cloud data shows a good matching with image data because hybrid IMU data is initialized by the result of bundle block adjustment of sequential image data. Each point of geo-referenced laser point data corresponds to a pixel of geo-referenced CCD image in the same coordinate system. In this research, 3D point cloud data takes on a color from the corresponding image pixels for textured DSM as shown in Figure 13. Figure 14 is ortho mosaic image which is constructed by using digital surface model and oriented images.

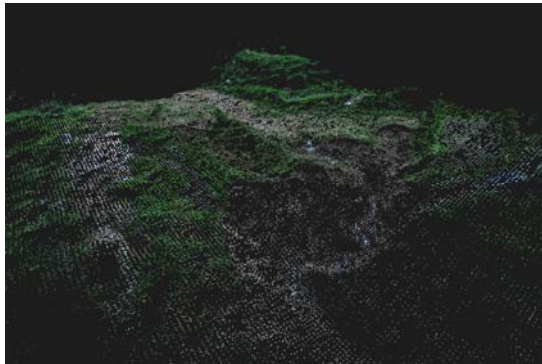


Figure 13. DSM



Figure 14. Ortho mosaic image

4.3 Vegetation Index

As the same as digital camera image, image processing is conducted for IR camera images as shown in Figure 15. After image orientation calculated in IR images, NDVI is calculated. Laser range data and IR camera images corresponds each other. Then, vegetation index is applied to digital surface model. 3D point cloud data takes on a color from the corresponding NDVI images. Figure 16 shows 3D point cloud data with NDVI.

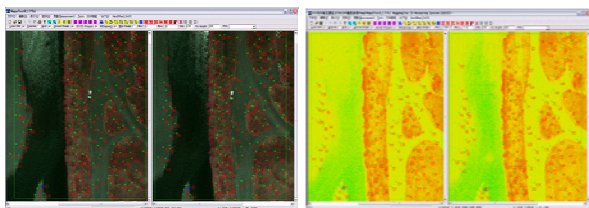


Figure 15. IR image processing

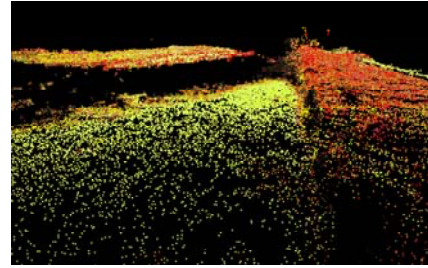


Figure 16. 3D point cloud data with NDVI

4.4 Accuracy assessment

In this study, multi sensors are integrated for mapping, so it is difficult to verify the origin of errors. Therefore, the accuracy assessment of DSM is done by comparing with control points from oriented images. Control points are selected 10 feature points such as object corners or conspicuous feature. As a result, average error of digital surface model is approximately 10cm to 30cm as shown in Table 3. The accuracy of the hybrid IMU is also estimated by the this mapping accuracy.

No.	Control point from Image			DSM			Error		
	(X)	(Y)	(Z)	(X)	(Y)	(Z)	(X)	(Y)	(Z)
1	-11184.877	-25630.253	42.755	-11184.696	-25630.836	42.915	0.181	0.583	0.160
2	-11185.471	-25622.727	42.952	-11185.557	-25622.789	42.971	0.086	0.062	0.019
3	-11167.603	-25670.474	42.391	-11168.282	-25670.312	42.406	0.679	0.162	0.015
4	-11177.107	-25634.721	42.704	-11177.262	-25634.918	42.523	0.155	0.197	0.181
5	-11152.866	-25641.753	42.029	-11152.172	-25641.036	42.071	0.694	0.717	0.042
6	-11176.511	-25625.571	42.824	-11176.467	-25625.426	42.767	0.044	0.145	0.057
7	-11153.911	-25643.823	42.534	-11154.375	-25643.041	42.075	0.464	0.782	0.459
8	-11150.564	-25631.724	42.340	-11150.887	-25631.869	42.296	0.323	0.145	0.044
9	-11176.771	-25635.344	43.992	-11176.394	-25635.308	44.082	0.377	0.036	0.090
10	-11186.666	-25631.657	44.289	-11186.417	-25631.888	44.202	0.249	0.231	0.087
Ave. Error							0.325	0.306	0.115

T

Table 3. Accuracy of digital surface model

5. CONCLUSION

In conclusion, all the inexpensive sensors, laser scanner, CCD cameras, IMU, and GPS are integrated for mapping. Digital surface model and ortho mosaic images are constructed by using all the sensors. In this research, a new method of direct geo-referencing for laser range data and CCD images by the combination of GPS/IMU and bundle block adjustment by the Kalman filter is proposed. Because of the aiding accumulation of error of the Kalman filter by bundle block adjustment, geo-referenced laser range data and CCD images are overlapped correctly in the common world coordinate system automatically. The data resolution and accuracy of mapping is good enough compared with satellite remote sensing and aerial remote sensing. All the sensors and equipments are assembled and mounted on an UAV in this experiment. This paper focus on how integrate these sensors with mobile platform. Finally, precise trajectory of the sensors is computed as hybrid IMU and it is used to construct digital surface model with texture and vegetation index. In the future, small UAV system is also applied with selected sensors for certain observation target.

References from Journals:

Nagai, M., Shibasaki, R., 2006, Robust Trajectory Tracking by Combining GPS/IMU and Continual CCD Images, Proceedings

of the Twenty-Fifth International Symposium On Space Technology and Science Kanazawa, pp.1189-1194.

Kunii, Y., Chikatsu, H., 2001, Application of 3-Million Pixel Armature Camera for the 3D Modeling of Historical Structures, Asian Journal of GEOINFORMATICS Vol. 2, No. 1, pp.39-48.

Shapiro, R., 1987, Direct linear transformation method for three-dimensional cinematography”, Res. Quart. 49, pp.197-205.

Kumagai, H., Kubo, Y., Kihara, M., Sugimoto, S., 2002, DGPS/INS/VMS Integration for High Accuracy Land-Vehicle Positioning”, Journal of the Japan Society of Photogrammetry and Remote Sensing, vol.41, no.4 pp.77-84.

Kuamgai, H., Kindo, T., Kubo, Y., Sugimoto, S., 2000, DGPS/INS/VMS Integration for High Accuracy Land-Vehicle Positioning, Proceedings of the Institute of Navigation, GPS-2000, Salt Lake.

Chen, T., Shibasaki, R., Murai, S., 2003, Development and Calibration of the Airborne Three-Line Scanner (TLS) Imaging System, Journal of the American Society for Photogrammetry and Remote Sensing PE&RS, vol.69, No.1,pp71-78.

References from Books:

Takagi, M., Shimoda, H., 2004, Handbook of image analysis, University of Tokyo Press.

Acknowledgement:

This research work is supported in part by the River Fund in charge of the Foundation of River and Watershed Environment Management (FORREM), Japan.

